stantial advance in the solution of the exciton complexes. The success of this method is again due to the fact that the interparticle potential is totally included in the zero order Hamiltonian H' and none of its terms appears in the remaining Hamiltonian H_1' used as perturbation. The development of this method to apply to other complicated observed complexes is in progress.

ACKNOWLEDGMENTS

I am very grateful to Professor A. A. Frost and Dr. A. Veillard for stimulating discussions. The computations have been carried out at the Computer Center of Cronenbourg, Strasbourg. I wish to thank Professor G. Monsonego, director of the computer center, for his valuable encouragement.

*Research Group associated to the CNRS France.
[1]S. G. Elkomoss, Phys. Rev. B 4, 3411 (1971).
[2]C. L. Pekeris, Phys. Rev. 112, 1649 (1958); 115, 1216 (1959).
[3]A. A. Frost, M. Inokuti, and J. P. Lowe, J. Chem. Phys. 41, 482 (1964).
[4]A. A. Frost, Theoret. Chim. Acta (Berlin) 1, 36 (1962).
[5]A. A. Frost and J. C. Patel, in *Quantum Theory of Atoms, Molecules, and Solid State* (Academic, New York, 1966), p. 147.
[6]P. S. C. Wang, J. Chem. Phys. 47, 2229 (1967).
[7]K. Jug, Theoret. Chim. Acta (Berlin) 7, 167 (1967).
[8]G. Munschy, J. Phys. (Paris) 28, 307 (1967).
[9]R. R. Sharma, Phys. Rev. 170, 770 (1967).
[10]R. R. Sharma and S. Rodriguez, Phys. Rev. 159, 649 (1967).
[11]B. Stebe and S. G. Elkomoss, J. Phys. (Paris) (to be published).
[12]P. Pluvinage, Ann. Phys. (Paris) 5, 145 (1950).
[13]P. Pluvinage, J. Phys. (Paris) 12, 789 (1951).
[14]P. Walsh and S. Borowitz, Phys. Rev. 115, 1206 (1959).
[15]P. Walsh and S. Borowitz, Phys. Rev. 119, 1274 (1960).
[16]P. Walsh, Westinghouse Electric Corp. Research Report No. BL-R-8-0089-6A6-1, 1958 (unpublished).
[17]S. G. Elkomoss, J. Phys. Chem. Solids 33, 750 (1972).
[18]H. Haken, Z. Naturforsch. 9a, 228 (1954); in *Halbleiter Probleme*, Vol. I, edited by W. Shottky (Vieweg, Braunschweig, 1954), p. 72; in *Halbleiter Probleme*, Vol. II, edited by W. Shottky (Vieweg, Braunschweig, 1955), p. 1; J. Phys. (Paris) 17, 826 (1956); and J. Phys. Chem. Solids 8, 166 (1959).
[19]E. Hylleraas, Z. Physik 54, 347 (1929).
[20]M. Abramowitz, *Tables of Bessel-Clifford Functions of Orders Zero and One*, Natl. Bur. Stds., Applied Mathematics, Series 28 (U.S. G.P.O., Washington, D.C., 1953).
[21]D. C. Reynolds, C. W. Litton, and T. C. Collins, Phys. Status Solidi 9, 645 (1965); 12, 3 (1965).
[22]D. C. Reynolds, C. W. Litton, and T. C. Collins, Phys. Rev. 156, 881 (1967); 177, 1161 (1969).
[23]D. C. Reynolds, in *Electronic Structures in Solids* (Plenum, New York, 1969), p. 110.
[24]J. P. Chandler, Physics Dept., Indiana University, Bloomington, Ind.; Program SIMPLEX QCPE 67, Chemistry Dept., Indiana University.
[25]J. J. Hopfield and D. G. Thomas, Phys. Rev. 122, 35 (1961).

PHYSICAL REVIEW B VOLUME 6, NUMBER 10 15 NOVEMBER 1972

Strain-Dependent Electron Paramagnetic Resonance and Spin-Valley Coupling of Shallow Triplet Sn Donors in GaP

F. Mehran, T. N. Morgan, R. S. Title, and S. E. Blum
IBM Thomas J. Watson Research Center, Yorktown Heights, New York 10598
(Received 21 April 1972)

We describe electron-paramagnetic-resonance studies of shallow tin donors in GaP under applied uniaxial stress. Because of the X_3 symmetry of the conduction-band minima relative to a Ga site, the Sn donor states are "orbital" triplets whose components correspond to the three valleys, with the sixfold degeneracy (including spin) split by a weak spin-valley coupling. The valleys are mixed also by the angular momentum operator of the Zeeman Hamiltonian with a small effective intervalley g factor g_L. From the stress dependence of the resonance we have determined directly the one-valley g factors $g_\perp = 1.997 \pm 0.001$ and $g_\parallel = 1.991 \pm 0.003$ and the intervalley g factor $g_L = 0.010 \pm 0.002$. This is the first time that these parameters are determined for GaP. In addition, we deduce the value $(4.8 \pm 0.7) \times 10^{-4}$ for the rms value of random strain and 5.2 ± 0.4 eV for the deformation potential Ξ_u^* of the bound state.

I. INTRODUCTION

Electron-paramagnetic-resonance (EPR) studies of electrons at donor sites in semiconductors have been very useful in yielding information concerning the wave functions of the donor states and band structure of semiconductors.[1] The wave functions of the ground states of the donors for which EPR

has been performed to date have, with one exception, interstitial Li and Si,[2] all involved orbital singlets. This includes measurements on the elemental semiconductors Si and Ge [1] and the compound semiconductors SiC,[3] GaAs,[4] InSb,[5] InAs,[6] and GaP.[7] In this paper we shall describe EPR studies on the group-IV donor Sn in GaP. The group-IV donors (substitutional at Ga sites) differ from the previously studied[7] group-VI donors (substitutional at P sites) in GaP in having ground states which are orbital triplets.[8]

For semiconductors with three conduction-band valleys at the ⟨100⟩ zone edges, the representation X_1 or X_3 to which the conduction-band minima belong, depends upon the choice of the origin of the coordinate system.[8] For the origin at the P site in GaP the conduction-band minima have X_1 symmetry, and the ground state of an electron bound to an impurity at that site is an orbital singlet composed of all three valleys. For the origin at a Ga site, the conduction-band minima have X_3 symmetry, so that the states of the electrons bound to Ga-site impurities are not mixed by the impurity potential and the electrons occupy orbital triplets. This difference can be determined from EPR measurements on the bound donor electrons.

The spin resonance of group-VI donor electrons in GaP has been studied previously[7] and is well understood. Since the ground state is an orbital singlet, it exhibits an isotropic g factor which is an average of the components of the single-valley g tensor parallel and perpendicular to the valley axes,[9]

$$g_0 = \tfrac{1}{3} g_{\parallel} + \tfrac{2}{3} g_{\perp} .$$

The threefold degeneracy of the group-IV donors can be lifted by either spin-orbit (= spin-valley)[10] splitting or by application of uniaxial stress that removes the equivalence of the three conduction-band minima or alters the shape of the minima. Because of the electron spin the "spin-orbit" interaction splits the six states derived from the triplet into a quartet and a lower-lying doublet. This splitting is relatively small and may be masked by internal random strain in the samples. A large uniaxial stress applied in an appropriate direction can overcome the effects of the internal strains, and makes it possible to observe EPR signals. The observation by Haraldson and Ribbing[11] of group-IV donor resonances in an externally unstressed-polycrystalline-GaP sample presumably resulted from the presence of large nonrandom internal strains in their materials.

II. THEORY

A. Introductory Remarks

The wave function for the ground state of an electron bound to an Sn donor has a $1s$-like envelope function. The z component (z valley) of such a $1s$-like state can be written

$$\psi_z(r) = F_{1s}(z, r) u_z(r) \sin k_0 z \qquad (1)$$

(with similar expressions for the x and y components), where $u_z(r) \sin k_0 z$ denotes the Bloch function of the z valley at $k_0 = 2\pi/a$, and $F_{1s}(z, r)$ is an envelope function satisfying the effective-mass equation.[12] Such a triplet state possesses both a nonvanishing "orbital" (intervalley) g factor g_L and a finite "spin-orbit" (spin-valley) interaction,[10] although both may be small because of the periodic factor $\sin k_0 z$. Thus, the theory of spin resonance of group-IV donors in GaP must include this orbital g factor as well as the mixing among the six nearly degenerate states (including spin) split by the small spin-orbit interaction.

Because of the orbital degeneracy, uniaxial strains along the ⟨100⟩ axes, which split the energies of the x, y, and z valleys, significantly alter the wave functions and g factors in the manner found by Feher *et al.*[13] for degenerate hole states in Si. In particular, if the random strains in the crystal produce valley splittings which are large compared to the spin-orbit splitting, they broaden the lines and destroy the resonance. In this case only after an external stress of sufficient magnitude is applied does the resonance reappear. In our analysis we shall derive the wave functions and g factors for an orbital triplet split by a weak spin-orbit coupling and perturbed by both random and externally applied ⟨100⟩-type strains. A similar analysis has recently been carried out by Watkins and Ham[2] in their resonance study of the doublet and triplet states associated with the interstitial donor Li in Si. The exceedingly small value which they found for the spin-orbit splitting factor ($\lambda \lesssim 0.05$ cm^{-1}) allowed them to make certain simplifying assumptions which are unjustified for our case.

B. Ideal Model

We begin with the basic model having three valleys (see Fig. 1) which are coupled by a weak spin-orbit interaction and of which one (the z valley) is separated from the other two by a uniaxial stress applied along an axis in the $(1\bar{1}0)$ plane. The perturbing Hamiltonian contains the two terms

$$\mathcal{H} = \mathcal{H}_{so} + \mathcal{H}_T \qquad (2)$$

describing the spin-orbit and applied-stress interactions, respectively.

The spin-orbit interaction term

$$\mathcal{H}_{so} = \lambda \vec{S} \cdot \vec{L} \qquad (3)$$

is conveniently rewritten, following Ham,[14] in terms of a fictitious angular momentum operator $\vec{\mathcal{L}} \propto \vec{L}$ defined by its nonvanishing matrix elements

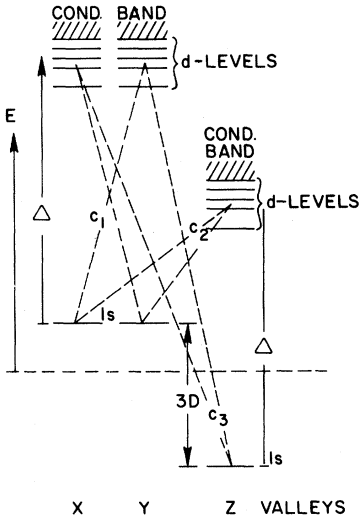

FIG. 1. Schematic diagram of the donor energy levels of the x, y, and z valleys under positive [001] stress. The labels c_i identify the nd states mixed with the $1s$ ground state by the local strain and Stark fields.

with respect to the functions ψ_x, ψ_y, and ψ_z,

$$\langle\psi_x|\mathcal{L}_z|\psi_y\rangle=\langle\psi_y|\mathcal{L}_x|\psi_z\rangle=\langle\psi_z|\mathcal{L}_y|\psi_x\rangle=-i. \tag{4}$$

Thus

$$\mathcal{H}_{so}=\lambda'\vec{S}\cdot\vec{\mathcal{L}}, \tag{5}$$

where the effective spin-orbit splitting factor is

$$\lambda'=g_L\lambda, \tag{6}$$

and g_L is the orbital g factor defined in terms of the usual angular momentum operator $\vec{L}$,[14]

$$g_L=i\langle\psi_x|L_z|\psi_y\rangle. \tag{7}$$

For the triplet states as defined by Eq. (1) the tensor g_L is isotropic. We note from Eqs. (4) and (5) that we may develop the theory in terms of $\vec{\mathcal{L}}$ and $\vec{S}$ in the usual way, provided we modify λ according to (6) and introduce an orbital g factor g_L from (7).

The interaction with the applied stress, which may be written

$$\mathcal{H}_T=D(3\mathcal{L}_z^2-\mathcal{L}^2)\quad, \tag{8}$$

raises the energies of the x and y components ψ_x and ψ_y by an amount D while depressing the z component by $2D$. The parameter D is

$$\begin{aligned}D&=\tfrac{1}{3}\Xi_u^*[e_{zz}-\tfrac{1}{2}(e_{xx}+e_{yy})]\\&=\tfrac{1}{3}\gamma_1\Xi_u^*(s_{11}-s_{12})T\equiv C(\theta)T\quad,\end{aligned} \tag{9}$$

where Ξ_u^* is the shear deformation potential for the donor state; e_{xx}, e_{yy}, and e_{zz} are the diagonal components of the strain tensor; s_{11} and s_{12} are cubic compliance constants; and $\gamma_1=[z^2-\frac{1}{2}(x^2+y^2)]/|\vec{R}|^2$ for stress along $\vec{R}=(x, y, z)$. Thus,

$$\gamma_1=\begin{pmatrix}1\\ \frac{1}{2}\\ -\frac{1}{2}\end{pmatrix}\text{for stress applied in}\begin{Bmatrix}\langle001\rangle\\ \langle112\rangle\\ \langle110\rangle\end{Bmatrix}\text{directions.} \tag{10}$$

In the Hamiltonian the two terms of Eq. (2) are of comparable magnitude (of order 1–10 meV), while the Zeeman term, described in Sec. II C, is much smaller. Therefore we solve the secular equation for (2) acting alone and treat the Zeeman term by degenerate-perturbation theory. For basis functions we use the set $|\mathcal{L}, S, M_{\mathcal{L}}M_S\rangle$, where $M_{\mathcal{L}}$ and M_S are the components of $\vec{\mathcal{L}}$ and $\vec{S}$ along the z cubic axis. Since $\mathcal{L}=1$ and $S=\frac{1}{2}$ remain good quantum numbers, we omit them and write only $|M_{\mathcal{L}}, M_S\rangle$.

Solving the secular equation for (2), we find that the sixfold-degenerate level splits into three doubly degenerate levels shifted in energy by

$$E_0=\tfrac{1}{2}\lambda'+D=\tfrac{1}{2}\lambda'[1+\tfrac{1}{3}(x+1)] \tag{11a}$$

and

$$E_\pm=\tfrac{1}{2}(-D-\tfrac{1}{2}\lambda'\pm\tfrac{1}{2}Q\lambda')=\tfrac{1}{4}\lambda'[-1-\tfrac{1}{3}(x+1)\pm Q]\,, \tag{11b}$$

where

$$Q=(x^2+8)^{1/2}\quad\text{and}\quad x=1+6D/\lambda'\quad. \tag{11c}$$

Figure 2 shows these three energies as functions of D. Upon application of the external magnetic field, each of these Kramers doublets splits into two levels whose separation at resonance equals the microwave energy $h\nu$. Since our experiments

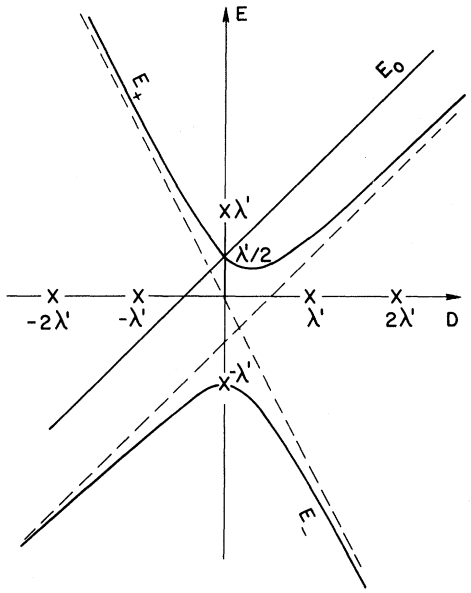

FIG. 2. Energy-level splitting of the ground state due to the combined effect of spin-orbit and deformation interactions as a function of the deformation parameter D.

were performed at low temperatures, they measured only the lowest of these doublets, that was described by E_- of (11b). The eigenstates $|E_- M_J\rangle$ which correspond to this energy and to the eigenvalues of the z component of the total angular momentum $M_J = M_{\mathcal{L}} + M_S = \pm \frac{1}{2}$ are

$$|E_-, \tfrac{1}{2}\rangle = a_- |1, -\tfrac{1}{2}\rangle - a_+ |0, \tfrac{1}{2}\rangle , \qquad M_J = \tfrac{1}{2} \tag{12a}$$

$$|E_-, -\tfrac{1}{2}\rangle = a_- |-1, \tfrac{1}{2}\rangle - a_+ |0, -\tfrac{1}{2}\rangle , \quad M_J = -\tfrac{1}{2} \tag{12b}$$

where

$$a_\pm = [\tfrac{1}{2}(1 \pm x/Q)]^{1/2} . \tag{13}$$

C. Zeeman Interaction

Since the orbital g factor g_L is not zero, the Zeeman Hamiltonian contains both orbital and spin parts:

$$\mathcal{H}_z = \mathcal{H}_{ZL} + \mathcal{H}_{ZS} . \tag{14}$$

Because of the modifications of the ψ_i produced by the local fields around the donor,[15] the orbital g tensor could be slightly anisotropic. However, the anisotropy of g_L due to this effect is extremely small and will be neglected in the present paper. Thus we write for the orbital Zeeman Hamiltonian

$$\mathcal{H}_{ZL} = \mu_B g_L \vec{\mathcal{L}} \cdot \vec{H} , \tag{15}$$

where μ_B is the Bohr magneton. The spin g tensor in any valley is slightly anisotropic relative to the valley axis because of spin-orbit coupling to higher bands.[9,16] Thus writing $g_\parallel$ and $g_\perp$ as the two components of the spin g tensor, the spin term becomes

$$\mathcal{H}_{ZS} = \mu_B \sum_i \left(g S_i H_i + g_\perp \sum_{j \neq i}{}' S_j H_j \right) P_i , \tag{16}$$

where $i, j = x, y,$ or z, and P_i is a projection operator on the orbital state ψ_i of the ith valley. These two terms combine to produce a Zeeman splitting of

$$\begin{aligned} h\nu &= \mu_B \{ (2a_-^2 g_L + a_+^2 g_\parallel - a_-^2 g_\perp)^2 H_\parallel^2 \\ &\quad + [2\sqrt{2}\, a_+ a_- g_L - a_+^2 g_\perp + a_-^2 \tfrac{1}{2}(g_\parallel - g_\perp)]^2 H_\perp^2 \}^{1/2} \\ &= \mu_B (g_\parallel'^2 H_\parallel^2 + g_\perp'^2 H_\perp^2)^{1/2} , \end{aligned} \tag{17}$$

where $H_\parallel^2 = H_z^2 = H^2 \cos^2\theta$ and $H_\perp^2 = H_x^2 + H_y^2 = H^2 \sin^2\theta$. Thus the components of the resulting g tensor $\tilde{g}'$ become

$$\begin{aligned} g_\parallel' &= 2a_-^2 g_L + a_+^2 g_\parallel - a_-^2 g_\perp \\ &= (1 - x/Q)(g_L - \tfrac{1}{2} g_\perp) + \tfrac{1}{2}(1 + x/Q) g_\parallel \end{aligned} \tag{18a}$$

and

$$\begin{aligned} g_\perp' &= 2\sqrt{2}\, a_+ a_- g_L - a_+^2 g_\perp + \tfrac{1}{2} a_-^2 (g_\parallel - g_\perp) \\ &= (4/Q) g_L - \tfrac{1}{4}(3 + x/Q) g_\perp + \tfrac{1}{4}(1 - x/Q) g_\parallel . \end{aligned} \tag{18b}$$

The sign ambiguity present for the g values determined from Eq. (17) has been resolved by noting that at zero stress (and for $g_\parallel = g_\perp \equiv g_s$), $g_\parallel' = g_\perp' = \frac{1}{3}(4g_L - g_s)$ as is found for a $p_{1/2}$ atomic level.

The dependence of the g factors on the stress T is conveniently expressed in terms of the parameter

$$K = D/\lambda' T = C(\theta)/\lambda' , \tag{19}$$

which depends on the ratio of the deformation potential to the effective spin-orbit splitting parameter of the donor state and also on the stress orientation through the factor γ_1 of Eq. (9). In terms of K we may write the stress-dependent factors in (18) as

$$Q = 2[2 + (3KT - \tfrac{1}{2})^2]^{1/2} \tag{20a}$$

and

$$x/Q = 2(3KT - \tfrac{1}{2})/Q = \pm [1 + 2/(3KT - \tfrac{1}{2})^2]^{-1/2} . \tag{20b}$$

For this model to explain the experimental results the asymptotic expansions of (18) for large stresses should fit the experiment in the range $|KT| \gg 1$. These expansions are, for $T > 0$,

$$g_\parallel' = g_\parallel - (g_s - g_L)/(3KT)^2 \tag{21a}$$

and

$$g_\perp' = -g_\perp + 2g_L/3KT + \tfrac{1}{2}(g_s + 2g_L)/(3KT)^2 , \tag{21b}$$

while for $T < 0$

$$g_\parallel' = -g_\perp + 2g_L + (g_s - g_L)/(3KT)^2 \tag{22a}$$

and

$$g_\perp' = \delta g + 2g_L/|3KT| - \tfrac{1}{2}(g_S + 2g_L)/(3KT)^2, \tag{22b}$$

where $g_s = \frac{1}{2}(g_\parallel + g_\perp)$ and $\delta g = \frac{1}{2}(g_\parallel - g_\perp)$. Thus, from measurements of the asymptotic g values and slopes at large stresses, $(KT)^2 \gg 1$, it should be possible to determine the parameters of Eqs. (21) and (22).

D. Random Strains

We have developed a quantitative theory of the consequences of random strains on the wave function and g factors. The details of this theory will be given in a future paper. Here, we give an outline of the theory and use the results. We have considered only $\langle 100 \rangle$-type strains belonging to the E irreducible representation of the T_d crystal group, which lift the degeneracies of one or more valleys, and have neglected any possible effects of $\langle 111 \rangle$-type random strains (transforming as T_2) which might mix different valleys. The latter have also been explored theoretically, but no experimental indications of their effects have been identified so far.

The ⟨100⟩-type random strains contribute two terms to the Hamiltonian—one $\mathcal{H}_\sigma$ which lifts the degeneracy of the x and y valleys and one $\mathcal{H}_\delta$ which does not. The latter, which we shall call the "parallel" strain, is of the form of Eq. (8) and can be included simply by altering the value of the coefficient D to

$$D' = D + \lambda' \delta \ , \tag{23}$$

where the dimensionless strain parameter δ is defined in accordance with Eq. (9). The former, which we shall refer to as the "perpendicular" strain, may be written

$$\mathcal{H}_\sigma = \tfrac{1}{2} \lambda' \sigma (\mathcal{L}_x^2 - \mathcal{L}_y^2) \ , \tag{24a}$$

where a second dimensionless strain parameter

$$\sigma = (E_u/\lambda')(e_{xx} - e_{yy}) \tag{24b}$$

measures its strength. This term has an off-diagonal matrix element of $\frac{1}{2}\lambda'\sigma$ between the states having $M_S = \pm 1$. The terms $\mathcal{H}_\delta$ and $\mathcal{H}_\sigma$ are partners in the two-dimensional irreducible representation E except for a factor of $2\sqrt{3}$ scaling σ. Thus, for random strains of this type the average values of δ^2 and σ^2 are related by

$$\langle \sigma^2 \rangle = 12 \langle \delta^2 \rangle \ . \tag{25}$$

In general, for a resonance to be experimentally observable, the contributions of the random strains to the Hamiltonian must be small compared to the energy separations between the two lowest doublets which these strains couple. Hence, by basing our calculation on assumptions about the smallness of only $\mathcal{H}_\sigma$, we can obtain solutions which are valid for any system in which the resonance can be measured. We observe in Fig. 2 that for most values of stress two levels lie close together with a separation of $\delta E \approx \lambda'$, while the third level moves away with increasing $|T|$ with a separation of $\delta E \approx 3|D|$. Hence, we have treated exactly the interaction between the two closer levels and include the remaining level by perturbation theory. Thus, for positive D ($T > 0$) the two highest energy levels, E_+ and E_0 of (11a) and (11b), are treated exactly and their mixing into the lowest level, the ground state E_-, is calculated by perturbation theory. For negative D ($T < 0$) the two lowest levels E_0 and E_- are treated exactly with the admixture of the third E_+ determined approximately.

For either positive or negative stress T the solutions corresponding to Eqs. (12) (but with the random strains included) may be written

$$\psi_{\pm 1/2} = \alpha \left| 0, \pm\tfrac{1}{2} \right\rangle + \beta \left| \pm 1, \mp\tfrac{1}{2} \right\rangle + \gamma \left| \mp 1, \mp\tfrac{1}{2} \right\rangle \ , \tag{26}$$

where the coefficients are functions of λ', D', and σ. The components of the g tensor calculated from the Zeeman Hamiltonian for this pair of functions are found to be the following functions of α, β, and γ:

$$g_\parallel' = (2\alpha^2 - 1) g_s + \delta g + 2(\beta^2 - \gamma^2) g_L \tag{27a}$$

and

$$g_\perp' = -(g_1^2 + g_2^2 + 2 g_1 g_2 \cos 2\phi)^{1/2} \ , \tag{27b}$$

where the signs are chosen to agree with (18) and

$$g_1 = \alpha^2 g_s - \delta g + 2\sqrt{2}\, \alpha\beta g_L \ , \tag{27c}$$

$$g_2 = 2\beta\gamma g_s + 2\sqrt{2}\, \alpha\gamma g_L \ , \tag{27d}$$

and $\tan\phi = H_y/H_x$.

We have determined the coefficients of Eq. (26) and have shown that the inclusion of the random-strain Hamiltonian does not alter Eqs. (21), the average g values for $T > 0$. For $T < 0$, however, Eqs. (22) are modified and give values (averaged over Gaussian distributions of δ and σ) of

$$g_\parallel' = -g_\perp + \epsilon g_L \left(2 - \frac{1}{3KT}\right) + \left(\frac{1+\epsilon}{2+\epsilon^2}(g_s - g_L) - \frac{\frac{1}{2}\epsilon g_L}{6\epsilon KT - 1}\right) \Big/ (3KT)^2 , \tag{28a}$$

$$g_\perp' = -(1 - \tfrac{1}{3}\epsilon^2)\left(1 + \tfrac{1}{3}\frac{\epsilon^2}{3KT}\right) g_s + \frac{\epsilon g_L}{3KT - \frac{1}{8}\sqrt{3}} - \frac{1}{4}\frac{g_s}{(3KT)^2} \pm g_2 \cos 2\phi , \tag{28b}$$

where

$$\epsilon = (2\langle \sigma^2 \rangle)^{-1/2} .$$

The analysis also predicts a very broad line (for $g_\perp'$, $KT \ll -1$) having a width of $\Delta g_\perp' \approx 0.2$. Hence, for $KT \ll -1$, $g_\perp'$ cannot be measured directly, but its value can be deduced from the angular dependence of the g factor as the field H is rotated through a small angle θ away from the z axis.

III. EXPERIMENTAL PROCEDURE

The single gallium phosphide crystal used in this study was grown by the liquid-encapsulation Czochralski technique[17,18] using a boric oxide encapsulant. Nitrogen at about 900 psi was used as the ambient. The tin-doped crystal was prepared by the direct addition of elemental tin to the gallium phosphide charge. Net carrier concentrations of $n = 4 \times 10^{17}$ was indicated by Hall measurements. The EPR measurements were all carried out at 4.2 °K in an X-band apparatus. The sample was placed in a piston made of Teflon which is sufficiently hard at 4.2 °K to transmit the stress. Lever arms were used to obtain mechanical advantage and keep the weights used to manageable levels. External uniaxial stresses were applied along the [001], [112], [110], and [111] directions in the $(1\bar{1}0)$ plane and variations of the g values were studied as functions of the magnitude and direction of the stress and the orientation of the

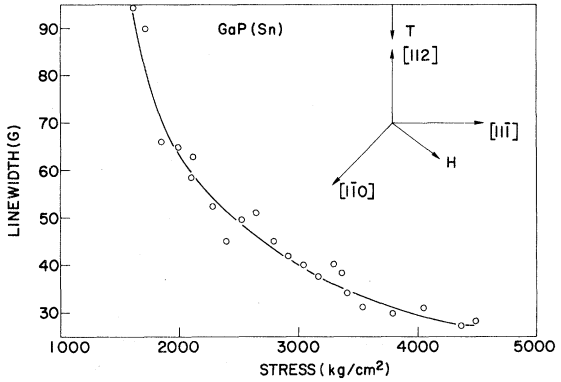

FIG. 3. Variation of the linewidth of the resonance signal with the magnitude of a uniaxial stress applied along the [112] axis.

magnetic field. All stresses were applied in the vertical direction while the magnetic field was kept in the horizontal plane.

IV. RESULTS AND DISCUSSION

A. Introductory Remarks

In this section we deduce the various parameters in the spin Hamiltonian from our experimental results. Throughout this procedure we assume that the "parallel"-internal-strain parameter δ in Eq. (23) is negligible compared to the applied strain. This is a reasonable assumption because the internal parallel strain deduced from the data is about 100 times smaller than the applied strain.

One noticeable feature of the observations is the improvement of the EPR signal as the stress is increased. The narrowing of the line is shown in Fig. 3 for a stress applied along the [112] direction. The broad lines at low values of externally applied stress are due to the presence of internal random strains in the crystals as described in Sec. IID. As the externally applied stress is increased, the g values become less sensitive to the internal strains and the linewidth approaches a limiting value which is probably principally due to the unresolved hyperfine interactions of the donor electron with the P^{31} nuclei within its orbit.

B. Strong Tetragonal Distortion: [001] Stress

For the stress applied along the [001] direction the parameter D defined in Eqs. (9) and (10) is positive ($\gamma_1 = 1$). In this case, the energy of the z valley is lowered while that of the x and y valleys is raised and, as shown in Fig. 2, in the absence of spin-orbit interactions the orbital triplet is split into a lower singlet and a higher doublet. The ideal model (Sec. II B) is adequate for the explanation of the stress dependence of the observed g factor. The observed g factor is $g_\perp'$, and its variation is described by Eq. (21b). The inclusion of the random strain in the Hamiltonian does not alter this equation. As expected, the spectrum for this case is isotropic with respect to the orientation of the magnetic field in the horizontal plane. Figure 4 shows the variation of the g factor versus the magnitude of a [001] stress with an arbitrary direction of the magnetic field in the horizontal plane. Figure 5 is a plot of the observed g values against $1/T^2$. The linearity of this dependence shows that the term in $1/T$ is negligible compared to the term in $1/T^2$ in Eq. (21b), which

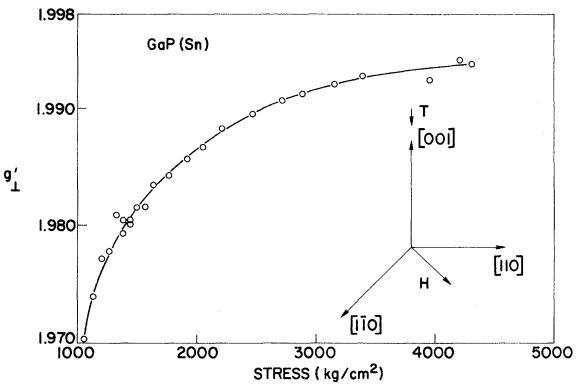

FIG. 4. Variation of $g_\perp'$ measured in the (001) plane with stress applied along the [001] direction.

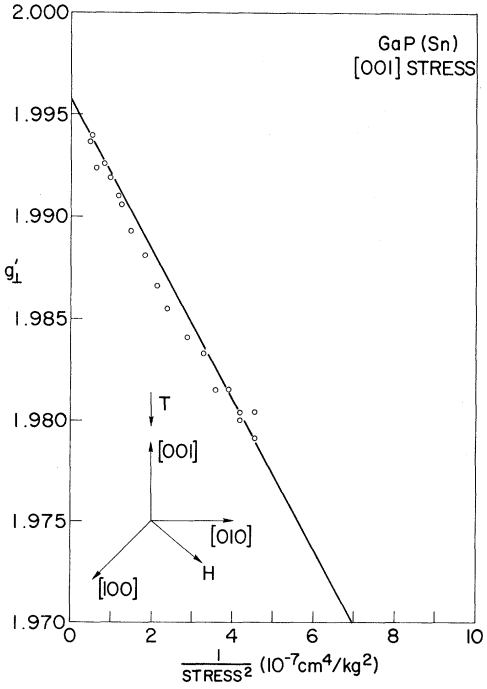

FIG. 5. Variation of $g_\perp'$ measured in the (001) plane vs $1/T^2$ for a [001] stress.

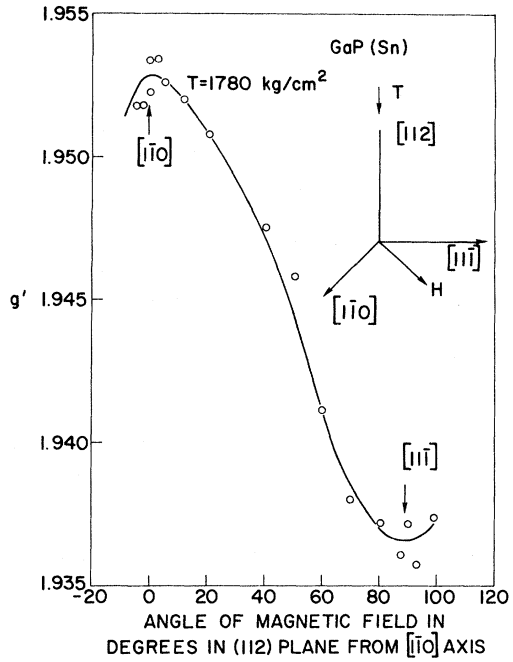

FIG. 6. Variation of g' with orientation of magnetic field in the (112) plane for a stress of 1780 kg/cm^2 applied along the [112] direction.

means that the parameter g_L is very small. The zero intercept of Fig. 5 gives $g_\perp = 1.996 \pm 0.001$, and the slope gives $(\frac{1}{2}g_s + g_L)/(3K)^2 = (3.8 \pm 0.1) \times 10^4$ kg^2/cm^4.

C. Weak Tetragonal Distortion: [112] Stress

For this direction of stress the parameter D is again positive although half as large as the [001] case ($\gamma_1 = \frac{1}{2}$). This means that a [112] stress is in effect a compression along the [001] axis. The appropriate formulas for this direction of stress are, therefore, Eqs. (21). When the magnetic field is along the [1$\bar{1}$0] direction the observed g factor is $g'_\perp$ of Eq. (21b), whereas with the magnetic field along the [1$\bar{1}$1] direction the observed g factor is $(\frac{2}{3}g'^2_\perp + \frac{1}{3}g'^2_\parallel)^{1/2}$, where $g'_\parallel$ is given by Eq. (21a). The spectrum should therefore be anisotropic. The experimental anisotropy is shown in Fig. 6 for a fixed value of applied stress. Figure 7 shows the variations of the observed g factors as functions of the magnitude of stress for the two directions of the magnetic field corresponding to the extrema of Fig. 6. The two curves in Fig. 8 are the plots of the g values versus $1/T^2$. Again, the linearity of these plots show that the $1/T^2$ terms in Eqs. (21) are dominant over the $1/T$ terms because of the smallness of g_L. The intercept of $g'_\perp$ (curve I) gives $g_\perp = 1.997 \pm 0.001$ and the slope gives $(\frac{1}{2}g_s + g_L)/(3K)^2 = (1.5 \pm 0.1) \times 10^5$ kg^2/cm^4. These values are in agreement, within the experimental uncertainty, with those of Sec. IV B. The slope of the [112] case is about four times the one for the [001] case as expected since $K_{[001]} = 2K_{[112]}$. The results from [112] stress are more reliable because the smaller value of K for this direction makes the second-degree term in $1/T$ even more important relative to the first-degree term, and the g values are observable over a wider range of stress. Curve II in Fig. 8 is $(\frac{2}{3}g'^2_\perp + \frac{1}{3}g'^2_\parallel)^{1/2}$. The zero intercept of this curve gives $(\frac{2}{3}g^2_\perp + \frac{1}{3}g^2_\parallel)^{1/2} = 1.995 \pm 0.001$ and the slope gives $(\frac{2}{3}g_s + \frac{1}{3}g_L)/(3K)^2 = (1.9 \pm 0.1) \times 10^5$ kg^2/cm^4. From a comparison of the two intercepts in Fig. 8 we deduce a value for $g_\parallel = 1.991 \pm 0.003$.

The isotropic g value observed for group-VI donors is $g_0 = \frac{1}{3}g_\parallel + \frac{2}{3}g_\perp$. Using our values for $g_\parallel$ and $g_\perp$, we calculate the isotropic g factor at

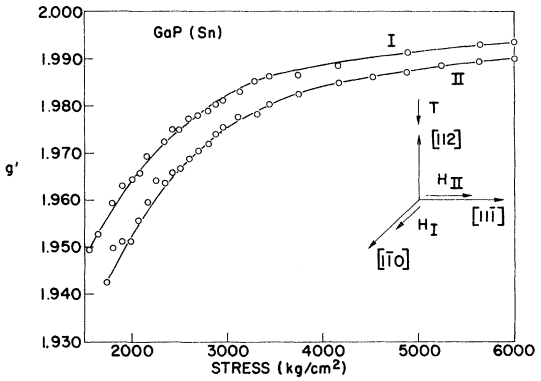

FIG. 7. Variation of g' measured along the [1$\bar{1}$0] axis (curve I) and along the [11$\bar{1}$] axis (curve II) with the magnitude of stress applied along the [112] direction.

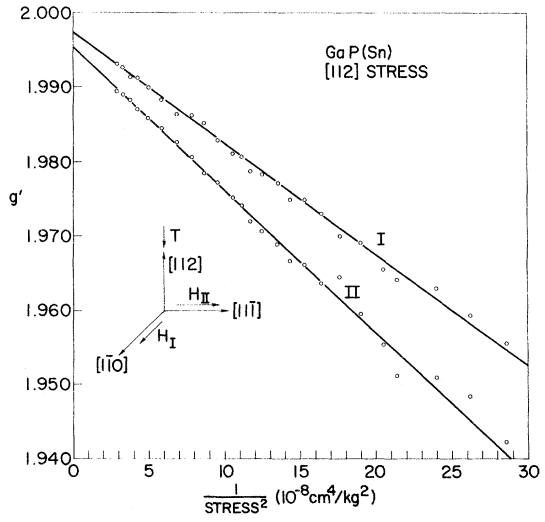

FIG. 8. Variation of g' measured in a [112] plane vs $1/T^2$ with stress applied along the [112] direction and field applied along [1$\bar{1}$0] (curve I) and along [11$\bar{1}$] (curve II).

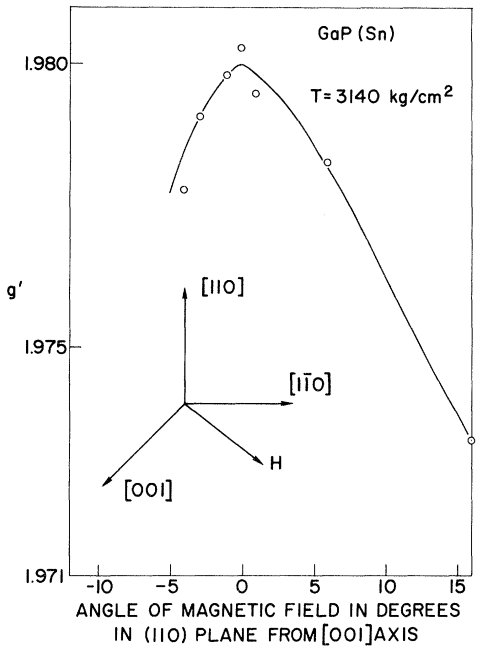

FIG. 9. Variation of g' with orientation of the magnetic field in a (110) plane for a stress of 3140 kg/cm^2 applied along the [110] direction.

4.2 °K, $g_0 = 1.995 \pm 0.002$. The g value for group-VI donors is given as[7] 1.9976 ± 0.0008. The data of Ref. 7 were obtained at 77 °K. To make a better comparison we measured the g value for GaP(Te) at 4.2° and obtained $g = 1.9935 \pm 0.0005$. The difference between the isotropic g value for infinite stress and the free electronic value of 2.0023 is due to the admixture of other bands into the conduction band by spin-orbit interaction,[9] and one expects that the infinite-stress value of $g_0' = \frac{1}{3}g_{\parallel}' + \frac{2}{3}g_{\perp}'$ for the group-IV donors should be the same as for the group-VI donors (the conduction-electron value).

D. Orthorhombic Distortion: [110] Stress

For this direction of stress the x and y valleys are depressed and the z valley is raised. This is equivalent to a tension along the [001] axis and the parameter D is negative ($\gamma_1 = -\frac{1}{2}$) [see Eqs. (9) and (10)]. The ideal model (Sec. II B) predicts Eqs. (22) for the high-stress variations of the observed g factors. The spectrum is anisotropic and only $g_{\parallel}'$ is observable. Figure 9 shows this anisotropy for a fixed value of applied stress. The $g_{\perp}'$ was not expected to be observed since from Eq. (22) $g_{\perp}' - \delta g \approx 0.003$. However, from the values of $g'(\theta)$ in the neighborhood of $g'(\theta \leq 15°)$ we can deduce $g_{\perp}' \approx 1.9$ using the formula $g'(\theta) = g_{\parallel}'^2 \cos^2\theta + g_{\perp}'^2 \sin^2\theta^{1/2}$. Here θ is the angle between the magnetic field and [001]. This large value for $g_{\perp}'$ and its lack of observability are both explained in terms of internal random strains in the crystal (Sec. II D). Figure 10 is a plot of $g_{\parallel}'$ versus the stress, and Fig. 11 is a plot of the $g_{\parallel}'$ versus $1/T^2$. Again the latter is linear, which indicates the dominance of the second-degree term in $1/T$ of Eqs. (22a) and (28a) and, hence, the smallness of g_L. The zero intercept of Fig. 11 is 1.989 ± 0.001. According to the ideal model (Sec. II B) in the absence of random strains this number should equal

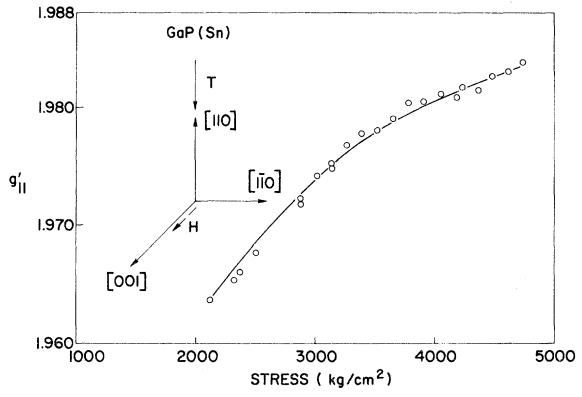

FIG. 10. Variation of $g_{\parallel}'$ measured along the [001] direction with the magnitude of a stress applied along the [110] direction.

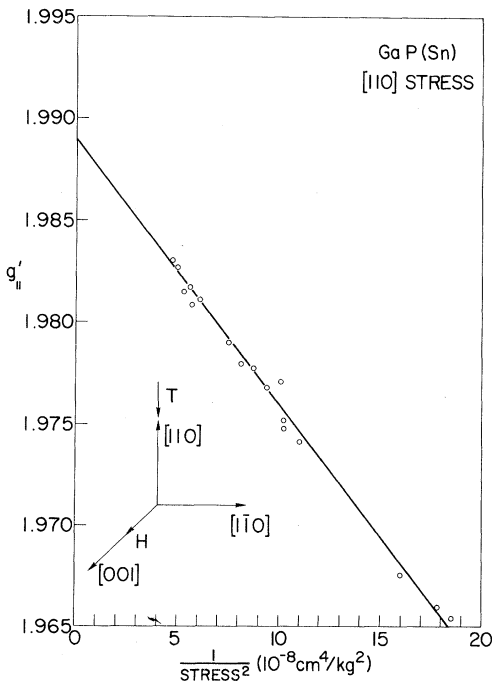

FIG. 11. Variation of $g_{\parallel}'$ measured along the [001] direction vs $1/T^2$ with the stress applied along the [110] direction.

$g_\perp - 2g_L$. Based on this model, therefore, $g_L = 0.004 \pm 0.001$. However, because of the random strains [Eq. (28a)] this value should be modified and to do this we need an estimate for the internal-random-strain parameter ϵ. We estimate this parameter by using the experimentally deduced value $g'_\perp = 1.9$ in Eq. (28b) and obtain $\epsilon = 0.39 \pm 0.02$. The corrected value for g_L is therefore $g_L = 0.010 \pm 0.002$. Our theoretical evaluations which will be described in a future paper show that the major contribution to the parameter g_L is due to the admixtures of the excited-d-envelope functions into the ground state by the local fields caused by the impurity.[15]

From the slopes of the plots in Fig. 8 we determine the parameter K:

$$K_{[001]} = D_{[001]}/\lambda' = (1.7 \pm 0.1) \times 10^{-3} \text{ cm}^2/\text{kg} .$$

The parameter λ' has been measured independently by Dean *et al.*[19] and is $\lambda' = 1.40 \pm 0.07$ meV. We can thus calculate D:

$$D_{[001] \text{ bound state}} = (2.4 \pm 0.2) \times 10^{-3} \text{ meV cm}^2/\text{kg} .$$

This compares with Balslev's[20] value for the conduction band:

$$D_{[001] \text{ conduction band}} = (2.9 \pm 0.3) \times 10^{-3} \text{ meV cm}^2/\text{kg}.$$

The deformation potential Ξ_u^* calculated from $D_{[001]}$ is $\Xi^* = 5.2 \pm 0.4$ eV for the bound state. The reductions in the value of the deformation potential from its band value is also caused by the admixtures of the d envelopes into the ground state and will be discussed in a future paper. From the parameter ϵ deduced above we can determine the rms value of the perpendicular internal-random-strain parameter σ: $\langle\sigma\rangle = 1.8 \pm 0.2$. The corresponding rms value for random strain from Eq. (24b) for the value of the deformation potential deduced above is $\langle\text{strain}\rangle = (4.8 \pm 0.7) \times 10^{-4}$.

E. Trigonal Distortion: [111] Stress

For this direction of stress no resonance signals were observed. This indicates that the deformation potential for this direction of stress is extremely small and as a result there is no appreciable intervalley mixing or splitting in the energies of the three valleys.

F. Summary of Results

We compile the measured and calculated parameters in this study. For the sake of completeness we include the relevant parameters measured by other workers:

$g_\parallel = 1.991 \pm 0.003$, $g_\perp = 1.997 \pm 0.001$,

$g_s = \frac{1}{2}(g_\parallel + g_\perp) = 1.994 \pm 0.002$,

$g_0(\text{calc}) = \frac{2}{3} g_\perp + \frac{1}{3} g_\parallel = 1.995 \pm 0.002$,

g_0 (from group-VI donors at 77 °K) $= 1.9976 \pm 0.0008$ (Ref. 7),

g_0 [from GaP(Te) at 4.2 °K] $= 1.9935 \pm 0.0005$,

$g_L = 0.010 \pm 0.002$, $\epsilon = 0.39 \pm 0.02$,

$\langle\sigma\rangle = 1.8 \pm 0.2$,

$\langle\text{internal random strain}\rangle = (4.8 \pm 0.7) \times 10^{-4}$,

$\lambda' = 1.40 \pm 0.07$ meV (Ref. 19), $\Xi_u^* = 5.2 \pm 0.4$ eV ,

$\Xi_u = 6.2 \pm 0.6$ eV (Ref. 20).

G. Conclusions

We have shown that the experimental observations in the strain-dependent EPR of GaP(Sn) can be explained in terms of an orbital-triplet donor state which is associated with the three conduction-band minima with X_3 symmetry. The three valleys at the X points are mixed by external- and internal-strain, spin-valley, and Zeeman-intervalley interactions. From the variations of the spectra with the magnitude and the direction of the applied stress we have deduced the parallel and perpendicular one-valley g factors, the intervalley g factor, the magnitude of the internal random strain, and the deformation potential for the bound state. These quantities are useful for the investigation of the nature of the band and bound states. In particular, the large intervalley g value and the reductions of the bound-state deformation potential below its band value indicate a large admixture of d states into the ground-state envelope function. These points will be further discussed in a future paper.

ACKNOWLEDGMENTS

The authors wish to acknowledge the technical assistance of C. J. Lent in growing the crystals, J. Keller in Hall measurements, G. Pigey in optical-emission analyses, J. M. Karasinski for x-ray alignments, A. Moldovan for cutting the crystals, and W. J. Fitzpatrick in the EPR measurements.

[1]For review articles on resonances in semiconductors, see G. W. Ludwig and H. H. Woodbury, in *Solid State Physics*, edited by F. Seitz and D. Turnbull (Academic, New York, 1962), Vol. 13, p. 223; B. Goldstein, in *Semiconductors and Semimetals, Physics of III-V Compounds*, edited by R. K. Willardson and A. C. Beer (Academic, New York, 1966), Vol. 2, Chap. 8, p. 189.

[2]G. D. Watkins and F. S. Ham, Phys. Rev. B 1, 4071 (1970).

[3]H. H. Woodbury and G. W. Ludwig, Phys. Rev. 124, 1083 (1961).

[4]W. Duncan and E. E. Schneider, Phys. Letters 7, 23

(1963).

[5]G. Bemski, Phys. Rev. Letters 4, 62 (1960).

[6]J. Konopka, Phys. Letters 26A, 29 (1967).

[7]R. S. Title, Phys. Rev. 154, 668 (1967).

[8]T. N. Morgan, Phys. Rev. Letters 21, 819 (1968).

[9]L. M. Roth, Phys. Rev. 118, 1534 (1960); L. M. Roth, B. Lax, and S. Zwerdling, *ibid.* 114, 90 (1959).

[10]The valley-dependent interactions should bear the more descriptive labels "intervalley" instead of "orbital" and "spin valley" instead of "spin orbit," though we shall sometimes refer to them by the more familiar names of atomic spectra.

[11]S. Haraldson and C. G. Ribbing, J. Phys. Chem. Solids 30, 2419 (1969).

[12]W. Kohn and J. M. Luttinger, Phys. Rev. 98, 915 (1955); W. Kohn, Solid State Phys. 5, 257 (1957).

[13]G. Feher, J. C. Hensel, and E. A. Gere, Phys. Rev. Letters 5, 309 (1960).

[14]F. S. Ham, Phys. Rev. 138, A1727 (1965). Note that the spin-orbit parameter λ' and the orbital g factor g_L as well as the effective deformation potential Ξ_u^* will also depend upon any dynamic Jahn–Teller mixing present in the ground state as discussed in this reference.

[15]T. N. Morgan, in *Proceedings of the Tenth International Conference on the Physics of Semiconductors, Cambridge, Mass.*, 1970 (U. S. AEC, Oak Ridge, Tenn., 1970), p. 266.

[16]H. Hasegawa, Phys. Rev. 118, 1523 (1960).

[17]S. W. Bass and P. E. Oliver, J. Crystal Growth 3, 286 (1968).

[18]S. E. Blum, R. J. Chicotka, and B. K. Bischoff, J. Electrochem. Soc. 115, 394 (1968).

[19]P. J. Dean, R. A. Faulkner, and S. Kimura, Phys. Rev. B 2, 4062 (1970).

[20]I. Balslev, J. Phys. Soc. Japan Suppl. 21, 101 (1966).